Underwater Spatial Field Monitoring with Small Scale Robots: An Experimental Study

Nathalie Bauschmann[1]
[1]Institute of Mechanics and Ocean Engineering, Hamburg University of Technology,
Eißendorfer Straße 42, 21073 Hamburg, Germany
E-mail(s): nathalie.bauschmann@tuhh.de

Abstract: Autonomous underwater vehicles (AUVs) can serve as efficient and cost-effective mobile sensor nodes for monitoring of underwater environments and construction sites such as marinas or nuclear storage ponds. In field exploration, the information collected by the AUV is used to construct a probabilistic field belief model of the environmental field. This can then be used to integrate an information metric into the path planning step. In this paper, a Gaussian Process-based field belief for a scalar, 2D underwater environmental field is investigated. The main contribution is the extensive experimental validation using real measurements. For testing purposes, a radiation field is mimicked using electro-magnetic carrier signals emitted by spatially distributed active beacons. Leveraging the attenuation of these signals underwater, the AUV measures the received signal strength. In literature so far, field exploration frameworks in the underwater domain are typically validated in experiments by simulating the field itself and the resulting measurements. While sensor noise can be integrated relatively easily, this still constitutes an over-simplification due to model imperfections. Moreover, this approach neglects other effects resulting from e. g. dynamic motion as the AUV interacts with the environment or field anomalies due to obstacles. Hence, an experimental investigation under realistic conditions is expected to deliver insights.

Keywords: Probabilistic field modeling, underwater robotics, Gaussian Process regression

Erschienen in Tagungsband 35. Forum Bauinformatik 2024, Hamburg, Deutschland, DOI: 10.15480/882.13531

1 Introduction

Autonomous underwater field exploration constitutes a promising task for mobile robots acting as mobile sensor nodes. With the continuous advances in miniaturization of computation technology, small-scale autonomous underwater vehicles (AUVs) are expected to play a prominent role in monitoring and exploration of environmental systems; an example of a small-scale underwater robot is depicted in Figure 1. Environmental 2D spatial fields of interest include radiation, oil concentration, temperature or total dissolved oxygen.

In field exploration, the information, i. e. measurements, collected by the AUV is used to construct a probabilistic field belief model of the environmental field. This information-theoretic metric can then be

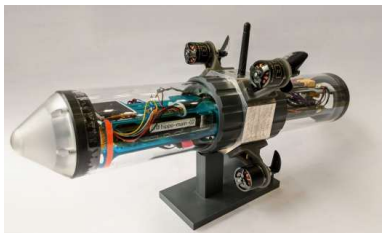

Figure 1: Example of a small-scale AUV used for spatial field mapping, the HippoCampus μAUV [7].

used in the AUV's path planning to save time during the mission. Consider the scenario of developing exploration algorithms for mobile underwater robots targeting environmental field monitoring, such as radiation fields. While investigating stationary spatial fields constitutes an obvious first step, their representation in submerged scenarios is challenging. This work studies the suitability of electromagnetic fields to mimic these fields. A focus lies on investigating potential disturbances, as antenna misalignments.

There has been extensive research on field exploration frameworks in the underwater domain. However, if these frameworks are validated experimentally, the field itself and the resulting measurements typically are simulated. A core reason being that time-constant fields are difficult to obtain. While sensor noise can be integrated relatively easily, this still constitutes an over-simplification, due to model imperfections. More importantly, this approach neglects other effects resulting from e. g. dynamic motion of the AUV.

One of the first works to deploy a field exploration algorithm in the real world is Cui et al. [1]. The authors map a 2D temperature field using a selective basis function Kalman filter. However, during the field experiments using four robots, they use simulated temperature measurement. Kemna et al. [2] use a log-Gaussian Process to map biological data, e. g. algae bloom. For the sake of simplicity, in field experiments in the subsequent publication [3], the authors use bathymetry data instead as a simple scalar field. This comes with the advantage of being fairly static in time and the possibility, to compose a ground truth model. A more in-depth field trial analysis is provided in [4]. Stankiewicz et al. use a Gaussian Process (GP) to model scalar environmental phenomena, namely dissolved oxygen measurements for water quality monitoring. Another example of using bathymetry data for field modeling is presented in [5].

In conclusion, the use of real-life measurement data in underwater field exploration frameworks is limited to physical, biological or chemical properties of large-scale outdoor environments. There are no examples of field belief modeling for confined environments such as nuclear storage ponds. This work explores the feasibility of using electro-magnetic (EM) carrier signals for underwater field exploration. Notably, received signal strength (RSS) data have been used in field modeling in other domains, e. g. using GP regression in an indoor environment in [6].

2 Modeling Electro-Magnetic Spatial Underwater Fields

In this work, we investigate the usage of 433 MHz EM carrier signal emitted by an active beacon to mimick a radiation field. Leveraging the attenuation of these signals underwater, a receiver antenna can measure the RSS. This section describes, first, the physical model of the radiation pattern and

attenuation of the antennas and, second, the hardware design of the measurement system consisting of the receiver and transmitter side. Finally, a GP-based field belief model is presented.

2.1 Electro-magnetic carrier signals underwater

Inspired by their usage in recent efforts in underwater localization [8], [9], omnidirectional dipole antennas emitting EM carrier signals of constant magnitude are used in this work. Omnidirectional dipole antennas display a doughnut-shaped radiation pattern. Therefore, the highest gain is achieved for receivers in the horizontal plane. The signal power varies with both the angle between a transmitter and receiver antenna, as well as the vertical distance between them. The 3D spatial attenuation characteristics of EM waves underwater, using omnidirectional antennas, are examined in detail by Kwak et al. [10].
The difference in EM wave power S_R on receiver side and EM wave power S_T on transmitter side is the RSS. This can be expressed as a function of the range R between receiver and transmitter antenna according to [8] as

$$\text{RSS} = S_\text{R} - S_\text{T} = -20 \log_{10} R - 20\ R\,\alpha \log_{10} e + \Gamma. \tag{1}$$

Here, Γ is an offset factor that represents antenna and environmental influences for the transmitter and α is the attenuation constant of the planar wave. The parameters Γ and α can be calculated explicitly if variables such as polarization loss factor, transmitting and receiving antenna gains and the attenuation factor are known. Alternatively, they can be determined through calibration, as described in [11].

2.2 Hardware Design

In the following, the hardware design is described. The transmitter unit consists of the Radiometrix™ USX2 module to generate the EM carrier signal in the 433 MHz band. As for the antenna, off-the-shelf dipole 2 dBi wifi antennas are used on the transmitter and receiver side. This is possible since the wavelength is shortened underwater. Therefore, the 433 MHz band sufficiently matches the characteristic wavelength of wifi systems in air, which operate at 2.4 GHz.
The receiver side consists of three main components: a commercial 2 dBi dipole wifi antenna, a modified Digital Video Broadcasting-Terrestial (DVB-T) USB dongle, and a single board computer (SBC), as depicted in Figure 2a. The NooElec™ NESDR Mini DVB-T USB dongle can process analog EM signals within a range of 24-1700 MHz, using software defined radio (SDR). After demodulation and analog digital conversion, the signals are transmitted as data sample to the SBC, a Raspberry Pi 4b, via USB interface. The SBC runs a fast Fourier transform on the samples to compute the RSS at the expected frequency in the power spectrum. A more in-depth description can be found in [11].

2.3 Field Belief Modeling

A common method for spatial modeling, also known in geostatistics as Kriging, is GP regression [12]. GP regression relies on two primary assumptions: spatial regularity, where measurements taken in close proximity are physically correlated, and Gaussian (zero-mean) measurement noise. The GP is completely defined by a mean function and its covariance matrix. While it is a non-parametric model, its performance is affected by hyperparameters, which are the kernel's parameters.

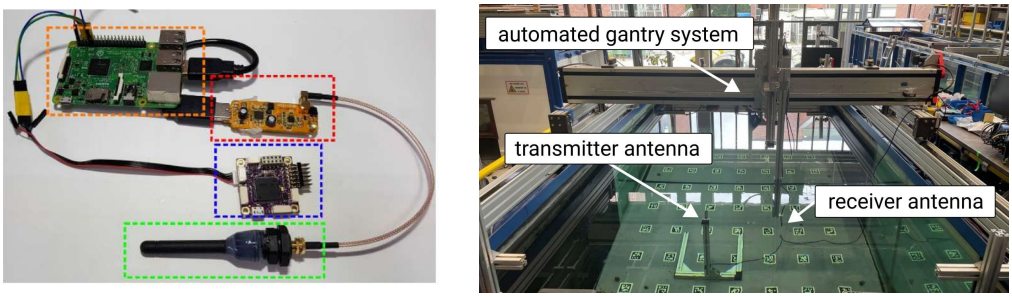

(a) (b)

Figure 2: (a) Components of EM receiver measurement setup: antenna (green), DVB-T dongle (red) and Raspberry Pi 4 single board computer (orange), (b) Experimental setup consisting of stationary transmitter beacon inside fresh water tank, receiver beacon on automated gantry system.

For the GP's kernel, a combination of the squared exponential function kernel [12] and a white noise covariance function is used, resulting in

$$k(\mathbf{x}, \mathbf{x}') = \sigma_f^2 \exp\left(-\frac{1}{2}\sum_{k=1}^{2}\frac{\left(x_{i,k} - x_{j,k}\right)^2}{l_k^2}\right) + \sigma_n^2 \delta_{\mathbf{x}_i,\mathbf{x}_j}, \tag{2}$$

with position $\mathbf{x} \in \mathcal{R}^2$ and the hyperparameter vector $\theta = \left[l_1, l_2, \sigma_f^2, \sigma_n^2\right]^\top$. Here, σ_f^2 is the signal variance, which determines the vertical scale of the function, and σ_n^2 is the variance of the noise. The parameters l_k are length scales in each dimension, which determine the level of correlation between measurements. Moreover, $\delta_{\mathbf{x}_i,\mathbf{x}_j}$ is the Kronecker delta function. The hyperparameters are optimized using the log-marginal likelihood as cost function [12] and the L-BFGS-B algorithm.

3 Analysis

The goal of the investigation is to, first, collect a 2D baseline field of the RSS values used as the ground truth in the following. Second, the sensitivity to possible error sources as they will occur with dynamic vehicle motions is investigated. Third, a *proof-of-concept* is shown to analyze how well a GP can capture the EM field's spatial characteristics. Finally, the results are discussed.
The experiments are conducted within a 2×4×1.5 m fresh water tank. A single stationary transmitter beacon is placed inside the tank. The receiver antenna is mounted on an automated gantry system, see Figure 2b.

3.1 Baseline

The RSS data is recorded in an evenly-spaced grid, with a distance of 5 cm between waypoints. At each waypoint, 80 measurements are recorded in a period of 3 s and the mean is taken. The results are depicted in Figure 3. It can be seen that the measured RSS value decreases with distance to the emitting beacon. However, interference effects roughly matching the ∼0.5 m wavelength can be observed.

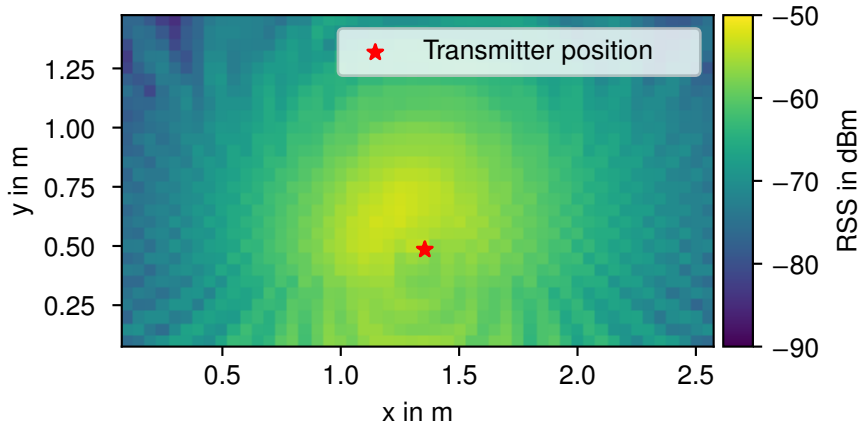

Figure 3: Baseline RSS measurement in fresh water tank, exhibiting interference effects.

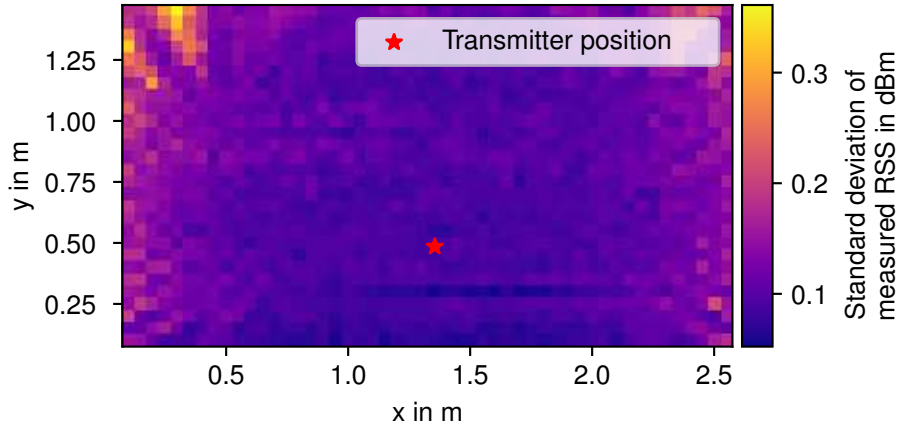

Figure 4: Standard deviation of baseline measurement.

3.2 Sensitivity to Alignment Errors

When the receiver antenna is deployed on an actual AUV, the dynamic motion is expected to affect the measurement. Even with extensive controller tuning, increasing forward thrust typically results in a pitch movement as well. Moreover, while the motion of the AUV is constrained to a 2D plane, depth control cannot be assumed to be perfect. Therefore, the effects of antenna misalignments, caused by relative tilts and vertical shifts between the receiver and transmitter antenna, are investigated in the following.

The RSS data is recorded on the same waypoint grid as in Section 3.1. Figure 5 depicts the error in RSS values compared to the baseline for antenna tilts of -20, -10, 10, and 20 degrees, as well as 10 cm and 20 cm vertical shift between the receiver and transmitter. It can be seen that the errors resulting from angle misalignment are comparatively small. However, for antenna tilts, an interesting effect can be observed. On one side of the transmitter antenna (right-hand side of Figure 5(a)-(d)), the measured RSS values *increase*, while on the other side, they decrease compared to the baseline. The maximum antenna gain and therefore the highest measured RSS value is expected for exact horizontal and angular alignment of antennas. Therefore, the increase in RSS in this setup can be

explained by an existing tilt or vertical offset in the baseline setup.
Moreover, the vertical displacement of the receiver antenna has a strong effect on the measured RSS value close to the transmitter antenna, as expected due to the doughnut-shaped radiation characteristics where the gain decreases above the antenna.

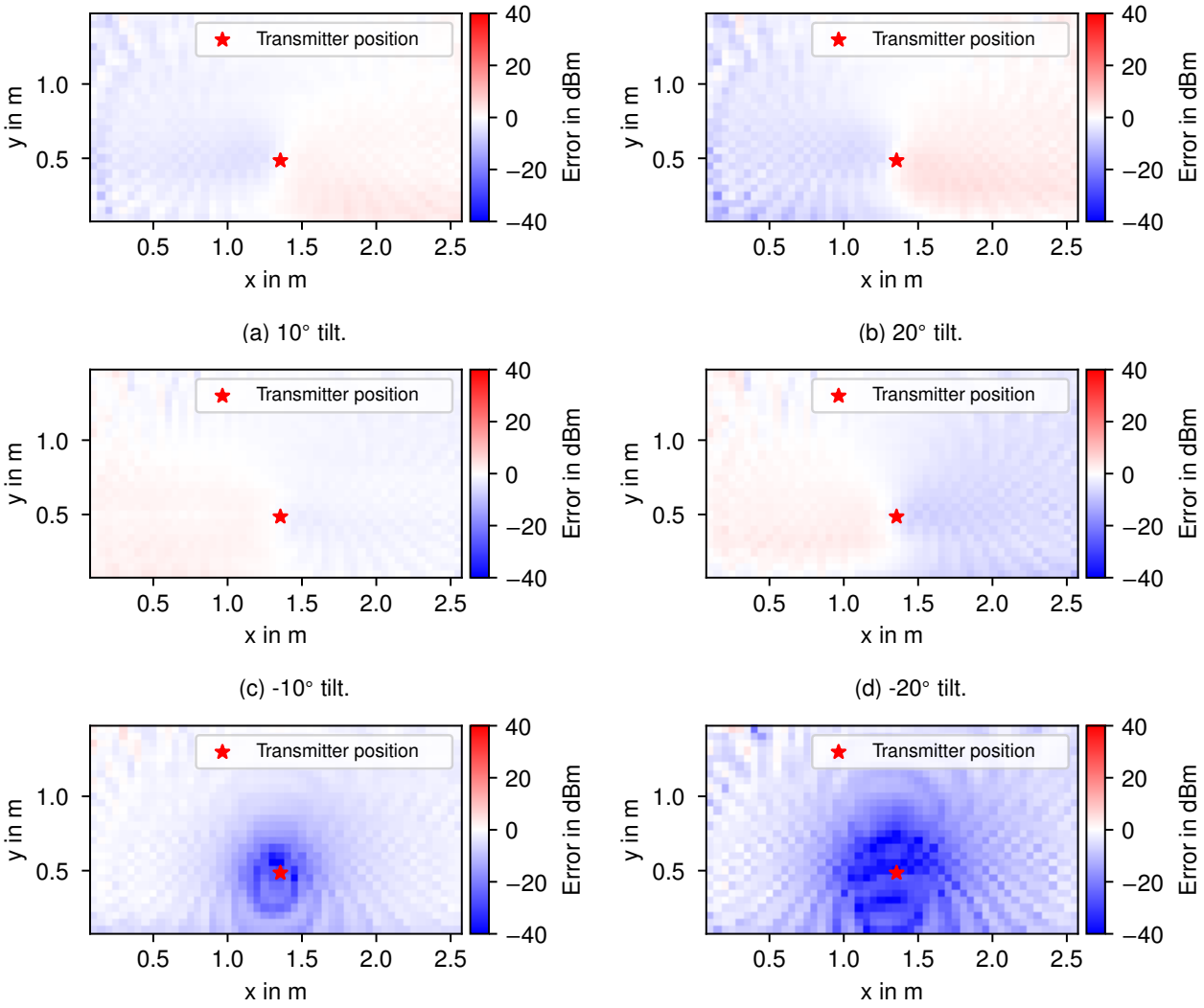

(a) 10° tilt.

(b) 20° tilt.

(c) -10° tilt.

(d) -20° tilt.

(e) 10 cm vertical shift.

(f) 20 cm vertical shift.

Figure 5: RSS error compared to baseline for different antenna misalignments. For angle shift, antenna is tilted around the x-axis.

3.3 Gaussian Process Regression Proof-of-Concept

As a first step towards leveraging EM measurements for underwater field exploration, general feasibility of modeling a 2D spatial RSS field using GP regression is demonstrated in the following. For this, 15 measurements are drawn at random positions. Figure 6 shows the predicted mean compared to the baseline measurement, with contour lines displayed at identical values. The results show a good fit for the absolute predicted RSS value, while the interference effects are not present in the model.

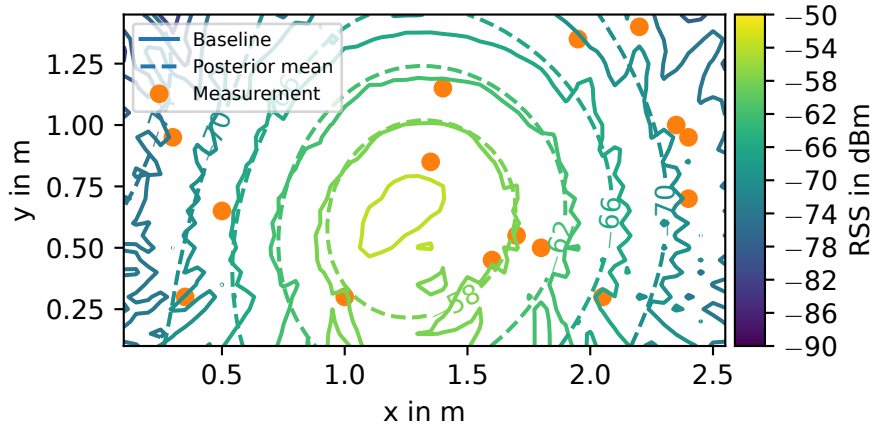

Figure 6: Predicted (dashed line) vs baseline (solid line) RSS values. 15 Measurements used for fitting the GP.

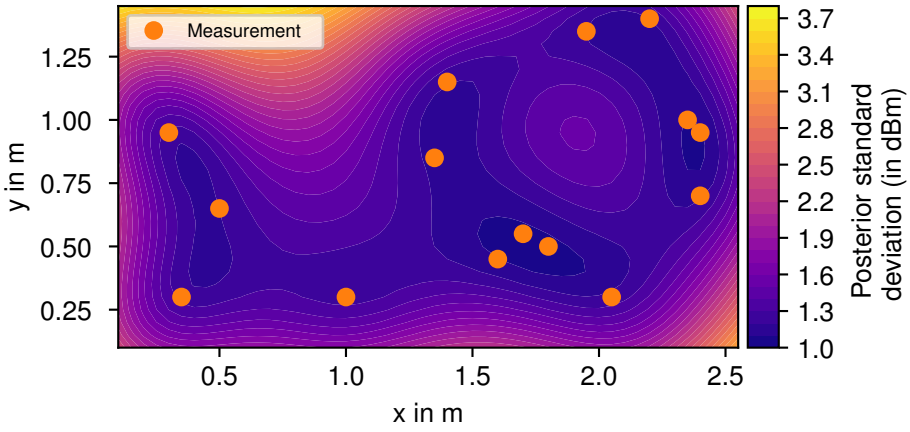

Figure 7: Uncertainty: posterior standard deviation of predicted RSS values after 15 measurements.

Moreover, Figure 7 depicts the uncertainty of the model, i. e. posterior standard deviation of each predicted RSS value. Around the measurements, the uncertainty is low, whereas in unexplored areas, the uncertainty is higher.

4 Conclusion

This work examines using EM carrier signals, precisely their attenuation, for underwater spatial field exploration. A stationary transmitter antenna emits a constant signal, while a mobile receiver antenna measures the RSS. The error analysis shows that the RSS measurements are very sensitive to vertical offsets between antennas in close proximity to the transmitter antenna. This is due to the radiation characteristics of the omnidirectional dipole antennas used. Comparatively, angle errors have less effect on the RSS. Modeling the RSS using a GP-based field belief was shown to be feasible.
As a next step, the measurement device will be deployed on a real robot, using this data to actively explore a spatial field. To overcome the shown sensitivity to angle and height misalignments, different antenna designs can be explored. Hemispherical antennas are promising due to their hemispherical radiation pattern. Alternatively, predicting errors using the robot's pose can be investigated.

References

[1] R. Cui, Y. Li, and W. Yan, “Mutual information-based multi-auv path planning for scalar field sampling using multidimensional rrt”, *IEEE Transactions on Systems, Man, and Cybernetics: Systems*, vol. 46, no. 7, pp. 993–1004, 2015.

[2] S. Kemna, J. G. Rogers, C. Nieto-Granda, S. Young, and G. S. Sukhatme, “Multi-robot coordination through dynamic voronoi partitioning for informative adaptive sampling in communication-constrained environments”, in *2017 IEEE International Conference on Robotics and Automation (ICRA)*, IEEE, 2017, pp. 2124–2130.

[3] S. Kemna, H. Heiarsson, and G. S. Sukhatme, “On-board adaptive informative sampling for auvs: A feasibility study”, in *OCEANS 2018 MTS/IEEE Charleston*, IEEE, 2018, pp. 1–10.

[4] P. Stankiewicz, Y. T. Tan, and M. Kobilarov, “Adaptive sampling with an autonomous underwater vehicle in static marine environments”, *Journal of Field Robotics*, vol. 38, no. 4, pp. 572–597, 2021.

[5] G. Flaspohler, V. Preston, A. P. Michel, Y. Girdhar, and N. Roy, “Information-guided robotic maximum seek-and-sample in partially observable continuous environments”, *IEEE Robotics and Automation Letters*, vol. 4, no. 4, pp. 3782–3789, 2019.

[6] N. Fung, J. Rogers, C. Nieto, H. I. Christensen, S. Kemna, and G. Sukhatme, “Coordinating multi-robot systems through environment partitioning for adaptive informative sampling”, in *2019 International Conference on Robotics and Automation (ICRA)*, IEEE, 2019, pp. 3231–3237.

[7] D. A. Duecker, N. Bauschmann, T. Hansen, E. Kreuzer, and R. Seifried, “Hippocampusx–a hydrobatic open-source micro auv for confined environments”, in *2020 IEEE/OES Autonomous Underwater Vehicles Symposium (AUV)*, IEEE, 2020, pp. 1–6.

[8] D. Park, K. Kwak, J. Kim, and W. K. Chung, “3d underwater localization scheme using em wave attenuation with a depth sensor”, in *2016 IEEE international conference on robotics and automation (ICRA)*, IEEE, 2016, pp. 2631–2636.

[9] D. A. Duecker, T. Johannink, E. Kreuzer, V. Rausch, and E. Solowjow, “An integrated approach to navigation and control in micro underwater robotics using radio-frequency localization”, in *2019 International Conference on Robotics and Automation (ICRA)*, IEEE, 2019, pp. 6846–6852.

[10] K. Kwak, D. Park, W. K. Chung, and J. Kim, “Underwater 3-d spatial attenuation characteristics of electromagnetic waves with omnidirectional antenna”, *IEEE/ASME Transactions on Mechatronics*, vol. 21, no. 3, pp. 1409–1419, 2016.

[11] D.-A. Duecker, A. R. Geist, M. Hengeler, *et al.*, “Embedded spherical localization for micro underwater vehicles based on attenuation of electro-magnetic carrier signals”, *Sensors*, vol. 17, no. 5, p. 959, 2017.

[12] C. E. Rasmussen and C. K. Williams, *Gaussian Processes for Machine Learning*. MIT Press, 2006.